Surface Science 286 (1993) 233–245
North-Holland

surface science

Interaction of CF_3I with Pt(111)

Z.-M. Liu, X.-L. Zhou, J. Kiss and J.M. White
Department of Chemistry and Biochemistry, University of Texas at Austin, Austin, TX 78712, USA

Received 2 October 1992; accepted for publication 16 December 1992

The interaction of CF_3I with Pt(111) has been studied using temperature programmed desorption (TPD), X-ray photoelectron spectroscopy (XPS), high resolution electron energy loss spectroscopy (HREELS) and work function change ($\Delta\phi$). CF_3I adsorbs molecularly at 85 K. Upon heating, all of the multilayer and part of the monolayer desorb at 100 and 168 K, respectively. The rest of the monolayer dissociates in two competitive channels. The first leads to CF_3 and atomic I and the second to CF_2 and halogens, with some evidence for IF. In the second, CF_2 radicals desorb promptly as they are formed ($\sim$ 150 K). When H(a) is present, reaction-limited HF desorption occurs at 220 K, a product attributed to decomposition of IF. In the presence of H(a), some CF(d3 is hydrogenated to form CF_3H which desorbs at 174 K. The remainder is stabilized; most desorbs as radicals at 623 K, but a small amount dissociates to produce CF_2, which desorbs with peaks at 750 and 850 K.

1. Introduction

Besides intrinsic interest, studying the surface chemistry of C_1 fluorocarbons is motivated by technological applications and environmental problems. This work was also motivated by our desire to compare CF_x and CH_x fragments on metal surfaces. While numerous commercial surface cleaning, etching, and lubricating processes involve fluorocarbons, little surface science has been reported on the simplest of these – the C_1 fluorocarbons. On well-characterized metals, CF_3I has been studied on Ni(100) [1,2], Ru(001) [3] and Ag(111) [4]. CF_3Cl, activated with low energy electrons and UV photons, has been studied on Pt(111) [5].

In this paper, we describe the thermal chemistry of CF_3I on Pt(111) as reflected in TPD, XPS, HREELS and work function ($\Delta\phi$) changes. In one dissociative channel, the weakest bond, C–I, is easily cleaved to form CF_3 and I, which, at low coverage, can occur even at 100 K. The CF_3 is either stabilized by the substrate, resulting in CF_3 desorption and dissociation around 600 K, or reacts in the presence of H(a) to form CF_3H, which desorbs at 174 K. There is a second dissociative channel, evidenced by low temperature CF_2 desorption, which is attributed to a competitive intramolecular reaction that forms adsorbed IF.

2. Experimental

The experiments were carried out in three different ultrahigh vacuum chambers, which, where comparisons were possible, gave consistent results. One chamber was equipped with temperature programmed desorption (TPD), high resolution electron energy loss spectroscopy (HREELS) and Auger electron spectroscopy (AES) facilities [6]. The second chamber was equipped for X-ray and ultraviolet photoelectron spectroscopy (XPS and UPS) and TPD [7]. The third chamber was equipped for TPD and AES.

The Pt(111) crystals were cleaned routinely by Ar^+ ion sputtering, oxidizing at 900–1000 in 5×10^{-8} Torr of oxygen to remove carbon, and annealing at 1200 K for several minutes to remove residual oxygen. The surface cleanliness was checked by AES or XPS. Trifluoromethyl iodide, CF_3I, (97%, Aldrich Chemical Company, Inc.) was purified by several freeze–pump–thaw cycles under liquid nitrogen. The dosing temperature

varied in different measurements as indicated below. CF_3I was dosed through a 3 mm diameter tube that terminated approximately 1 cm from the Pt(111) sample. Prior to dosing, the sample was turned away from the doser and the CF_3I pressure increased to $\Delta p = 5 \times 10^{-10}$ Torr at the ion gauge. To initiate dose, the sample was turned to face the doser. With this method of dosing, the absolute exposures in langmuir are unknown and only the relative exposures in dosing times are given.

During TPD (6 K/s), the sample was heated resistively and the temperature was monitored by a chromel–alumel thermocouple spot-welded to the back of the crystal. For XPS, a Mg Kα source was used to record F(1s) and I($3d_{5/2}$) core level spectra. The analyzer was set for 80 pass energy and 0.05 eV step size. HREELS measurements were carried out with a primary beam energy of 6.1×0.2 eV and a resolution of 10–12 meV full width at half maximum (FWHM). In the HREELS annealing sets described below, the sample was flashed to the desired temperature and cooled to 105 K before the spectra were taken. Secondary electron onsets, measured in He(I) UPS, were used to determine the surface work function changes ($\Delta\phi$).

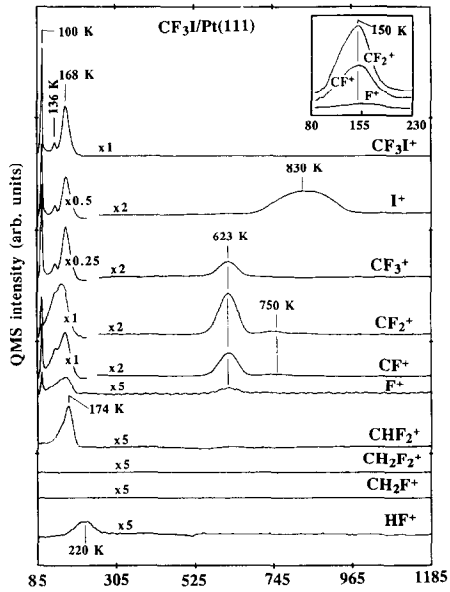

Fig. 1. TPD spectra of different species (indicated on each curve) for a multilayer CF_3I on Pt(111) dosed at 85 K. The TPD heating rate was 6 K/s. The inset shows the detailed CF_2^+, CF^+ and F^+ desorption features (with the parent CF_3I fragmentation subtracted).

3. Results

3.1. CF_3I/Pt(111)

3.1.1. TPD

Fig. 1 summarizes the TPD results for a multilayer of CF_3I dosed on Pt(111) at 85 K. The inset shows, for the temperature region from 85–230 K (see below), the detailed CF_2^+, CF^+ and F^+ desorption features (with the parent CF_3I fragmentation contribution subtracted). The relative abundances of ions derived from CF_3I fragmentation in our mass spectrometer are $CH_3I^+ : I^+ : CH_3^+ : CF_2^+ : CF^+ : F^+ = 22 : 32 : 77 : 8 : 11 : 1.2$, compared to 100:95:77:7:12:1.5 in the literature [8]. The profiles in the inset differ from CF_3^+. From these data and the mass fragmentation patterns of relevant species [8], we conclude that the TPD products, up to 1185 K, are parent CF_3I, HF, CHF_3, atomic I and CF_x ($x = 2, 3$) radicals. Note that for CHF_3 the most abundant fragment is CHF_2^+ ($m/e = 51$) and the parent ion, CHF_3^+ ($m/e = 70$), is barely detectable [8]. No other products were found, e.g. no evidence for CF_4, CH_2F_2, CH_3F, F_2, PtF_x ($x = 1$–4) and compounds containing two or more carbons.

Fig. 2 shows TPD spectra of parent CF_3I^+ as a function of dosing time (designated on each curve). No parent molecule desorbs for doses shorter than 200 s, indicating complete C–I bond dissociation. For longer doses, there is a peak at 168 K, which intensifies and saturates near 400 s. Above 400 s dose, an unsaturable peak, continuing the monotonic total peak area increase (fig. 6), grows in at 100, along with a small saturable peak at 136 K. We assign the peaks at 100 and 168 K to the multilayer and monolayer parent desorption, respectively. Here, we define one monolayer (ML) as the maximum exposure that gave no multilayer peak. Since the peak at 136 K increases significantly by introducing a small amount of atomic iodine (not shown) and since

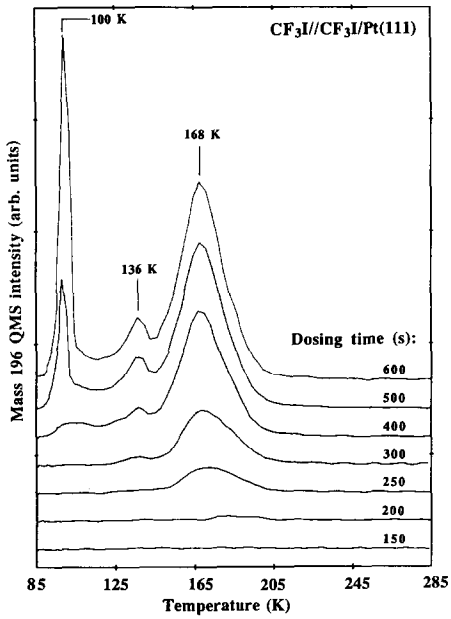

Fig. 2. TPD spectra of parent CF_3I for different CF_3I exposures (indicated as the dosing time on each curve) on Pt(111) at 85 K. The TPD heating rate was 6 K/s.

XPS data show noticeable CF_3I dissociation below 135 K, we attribute this peak to parent desorption influenced by atomic iodine.

Fig. 3 shows the TPD of CF_2^+ and its fragment CF^+ (with the parent CF_3I fragmentation subtracted) as a function of dosing time (designated

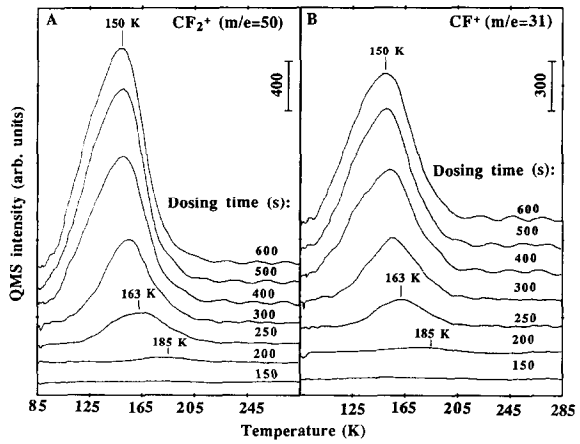

Fig. 3. TPD spectra of CF_2^+ and CF^+ (with the parent CF_3I fragmentation subtracted) as a function of CF_3I exposure. The experimental conditions were the same as in fig. 2.

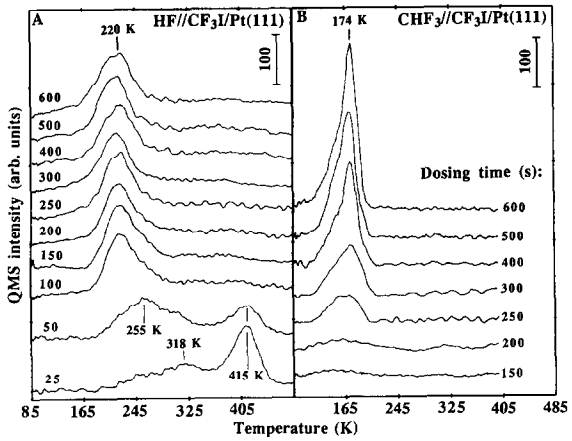

Fig. 4. TPD spectra of HF of CHF_3 as a function of CF_3I exposure. The experimental conditions were the same as in fig. 2.

on each curve). As for the parent, the CF_2^+ and CF^+ signals are negligible below 250 s. For a 250 s dose, both peak at 163 and, with increasing dose, they intensify and shift to 150 K. At saturation, the desorption onset is around 100 K. Since these two ion signals do not trace the parent desorption and since there is no CF_3^+ signal after CF_3I fragmentation is subtracted, we conclude that the 150 K peak is due to CF_2 desorption. Noting that there is CHF_3, but no CH_2F_2, desorption (nor CD_2F_2 in a coadsorption experiment with predosed D, see below), we conclude that these CF_2 radicals, unlike CF_3 fragments, desorb promptly when formed and have no opportunity to react with adsorbed surface hydrogen.

Fig. 4 shows the TPD of HF and CHF_3, monitored at $m/e = 20$ and 51 (CHF_2^+, the most abundant fragment of CHF_3), respectively, as a function of dosing time (designated on each curve). Unlike CF_2, HF appears at low doses. At 25 s, it desorbs with a broad peak at 318 K and a narrow peak at 415 K. At 50 s, the peak at 318 K shifts down to 255 K and the intensity of the 415 K peak decreases. Above 100 s, only one peak (220 K) is observed and it is saturated. Since atomic F on Pt(111) desorbs above 600 K [9], the detection of HF cannot be attributed to F desorption and subsequent reaction with background H_2. Rather, it is made on the surface involving surface H (from background) and F. The HF

desorption is reaction-limited because dosed molecular HF on Pt(111) desorbs at lower temperature (130 K [10]). While the reaction of surface H with F, which might be released from IF (see below) dissociation, can account for the low temperature HF desorption peak, the origin of high temperature HF is not clear. We speculate that CHF_x ($x \leq 2$) dissociation might account for it, since there is no surface hydrogen available above 400 K.

For CHF_3, there is only one desorption peak at 174 K, attributed to hydrogenation of CF_3 by H(a) adsorbed from the background, and it appears only above 200 s. When deuterium is coadsorbed, the same desorption feature for CDF_3 is observed (see below). Considering the fact that the adsorbed H(a) from background is still available at 220 but there is no more CF_3H formation and desorption, we suggest that there is some strongly bound CF_3 which desorbs at 623 K and is difficult to hydrogenate (see discussion section).

Fig. 5 shows TPD spectra of CF_x^+ ($x = 1$–3), the desorption of which sets in at about 550 K. All three exhibit peaks above 100 dose, and all become very strong at 250 s dose, where several other ions are just becoming observable. For CF_x^+ ($x = 1$ and 2), but not CF_3^+, there are two small peaks at 750 and 850 K. Noting that the most abundant fragment in the cracking pattern of CF_x is that of CF_{x-1} [3], we attribute the 623 K peaks to CF_3 radical desorption and the higher temperature peaks to CF_2 desorption. We should point out that surface F, presumably produced during CF_2(a) formation, is not detected (TPD, XPS, and HREELS, see discussion).

Fig. 6 summarizes TPD areas as a function of dosing time. For doses shorter than 200 s, there is no parent CF_3I desorption, no CHF_3 and no low temperature CF_2 desorption. The HF TPD area is roughly constant, which is understandable because the coverage of H adsorbed from background in each TPD run was roughly the same. Other species, atomic I (not including the low temperature peaks due to QMS fragmentation of parent CF_3I), high temperature CF_2 and CF_3, grow in from the lowest doses and approach saturation at 400 s.

For CF_3I doses shorter than 150 s, there is no parent desorption and the TPD area of atomic I increases linearly with the dose time with a slope

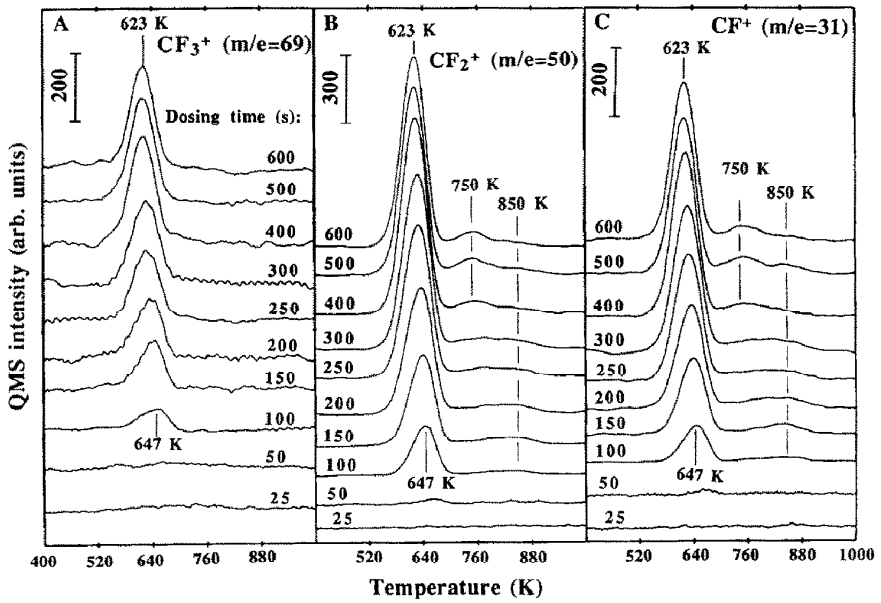

Fig. 5. TPD spectra of CF_3^+, CF_2^+ and CF^+ in the temperature region between 400 and 1000 K as a function of CF_3I exposure. The experimental conditions were the same as in fig. 2.

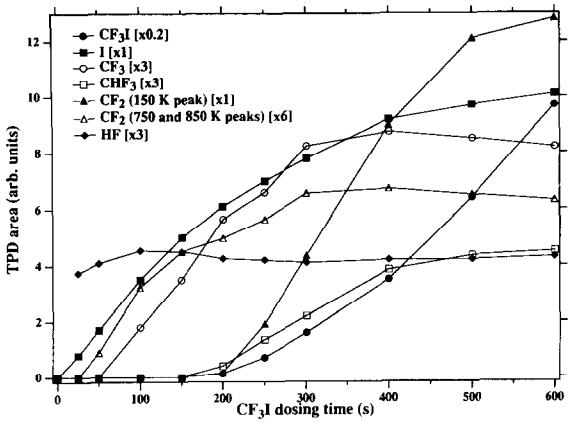

Fig. 6. TPD areas (from figs. 2–5) as a function of CF_3I dosing time.

of 0.035 units/s (arb. units, see fig. 6). Assuming a constant sticking coefficient of CF_3I, independent of coverage, we determine from the slope that the saturation I TPD area (~ 9.8 units, fig. 6) corresponds to a CF_3I dose time of 280 s. Fig. 2 indicates that saturation of the first monolayer CF_3I requires a dose of about 400 s. Thus, approximately 70% (0.7 ML) of the first monolayer CF_3I dissociates and 30% (0.3 ML) desorbs molecularly in TPD, which is in excellent agreement with XPS data (see below).

3.1.2. XPS

In order to obtain direct evidence for C–F and C–I bond cleavages, we measured XPS core level spectra of $I(3d_{5/2})$ and F(1s) for multilayer CF_3I prepared at 60 K and then flashed to different temperatures. The surface was recooled to 60 K prior to taking the spectra. The results are summarized in figs. 7 and 8. In passing, we note that varying the CF_3I coverage from submonolayer to multilayer at 60 K causes the $I(3d_{5/2})$ binding energy (BE) to shift upward by 0.1–0.15 eV, but has no effect on F(1s) position.

Fig. 7 shows the $I(3d_{5/2})$ XPS spectra (the temperatures to which the surface was flashed are indicated on each curve). Up to 90 K, only one symmetric peak at 620.4 with a FWHM of 1.66 eV is observed. It is assigned to molecular CF_3I. At 135 K, the intensity drops due to multilayer desorption. The peak broadens and shifts toward lower BE (619.9 eV), indicating C–I bond dissociation. With further heating, the $I(3d_{5/2})$ BE shifts further downward: 619.7 at 165 and 619.5 eV at 220 K. The broad $I(3d_{5/2})$ spectra at 135 and 165 K are readily deconvoluted into two peaks: one typical of molecular CF_3I at 620.4 and the other of atomic I(a) at 619.5 eV. From this, we estimate that the percentage of atomic I is 40 and 60%, at 135 and 165 K, respectively. Between 220 and 500 K, neither the intensity nor the position of $I(3d_{5/2})$ changes. At 1000 K, there is no longer any $I(3d_{5/2})$ signal, consistent with complete desorption of atomic I (fig. 1). From these results, we conclude that a significant amount of CF_3I dissociates to form CF_3(a) and I(a) at 135 K and no C–I bonds remain above 220 K. At 135 K, because the multilayer has desorbed, the $I(3d_{5/2})$ XPS area corresponds to 1 ML CF_3I. At 220 K, the $I(3d_{5/2})$ signal is due to atomic I, a dissociation product of CF_3I, and the XPS area is 70% of that at 135 K. This indicates that 0.7 ML CF_3I dissociates thermally, consistent with TPD results.

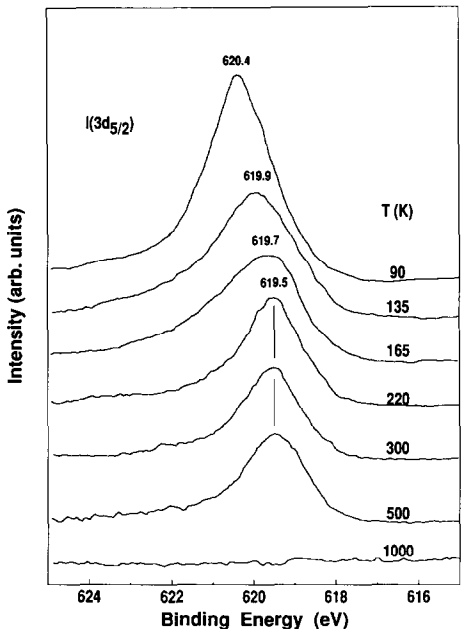

Fig. 7. $I(3d_{5/2})$ XPS spectra for a multilayer CF_3I on Pt(111) prepared at 60 K and then flashed briefly to the temperatures indicated on each curve. All XPS spectra were taken after recooling to 60 K.

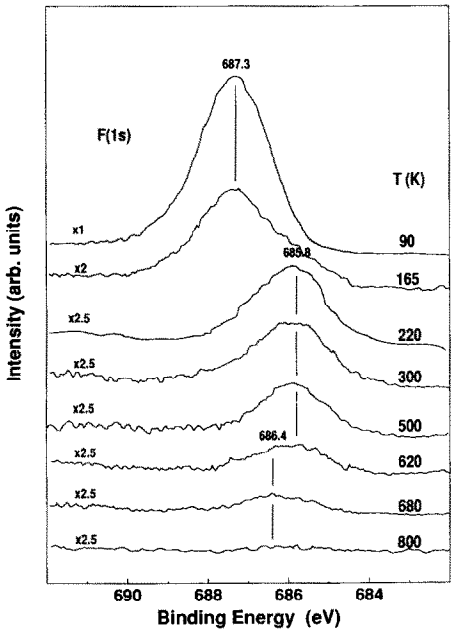

Fig. 8. F(1s) XPS spectra for a multilayer CF_3I on Pt(111) prepared at 60 K and then flashed briefly to the temperatures indicated on each curve. All XPS spectra were taken after recooling to 60 K.

Fig. 8 shows the comparable F(1s) XPS. At 90 K, F(1s) is symmetric with a BE of 687.3 eV. Upon heating to 135 K, the intensity decreases due to multilayer desorption. This F(1s) BE agrees with that for CF_3 on single crystal silicon [11], but lies below that (688.4 eV) for CF_3CL on Pt(111) [5]. Perhaps, compared to CF_3Cl, the stronger CF_3I–Pt interactions and the weaker C–I bond can account for the lower F(1s) BE. At 165 K the peak becomes asymmetric, and a shoulder at 685.8 eV appears. This finding is consistent with $I(3d_{5/2})$ spectra, indicating that, between 135 and 165 K, significant C–I bond dissociation occurs to form $CF_3(a)$. A more detailed examination of these spectra indicates a change in $I(3d_{5/2})$ at a lower temperature than F(1s), perhaps suggesting two forms of adsorbed $CF_3(a)$. No XPS signal at 684.6 eV, typical of F(a) [12], is observed. Upon heating to 220 IK, except for a shoulder, the peak at 687.3 eV disappears and the total F(1s) area decreases further. The 685.8 eV BE peak grows and dominates up to 500 K. Desorption of HF, CHF_3 and additional molecular CF_3I, as well as the formation of new surface species, account for the aforementioned changes. At 620 K, a 686.4 eV shoulder, assigned to CF_2, emerges. At 680 K, it becomes dominant. The decrease intensity at 685.8 eV is ascribed to CF_3 radical desorption and to dissociation to form $CF_2(a)$. Above 800 K, there is no F(1s) signal. These XPS results, together with HREELS data (see below), indicate that $CF_3(a)$ fragments, strongly interacting with the substrate, are stable up to 500 K. Most of them desorb as CF_3, but some dissociate to form $CF_2(a)$.

3.1.3. HREELS

HREELS results provide evidence for the following: (i) CF_3I adsorbs through the I atom. (ii) Upon heating to 177 K, some CF_3I desorbs and no C–I bonds remain in the adsorbates. (iii) Dissociation leaves $CF_3(a)$ fragments, which are the dominant CF_x species up to 500 K. (iv) Above 500 K, some CF_3 dissociates into $CF_2(a)$, which desorbs at a higher temperature. The results are shown in figs. 9 and 10.

Fig. 9 shows HREELS spectra at different CF_3I coverages (dosing time at 103 K shown on

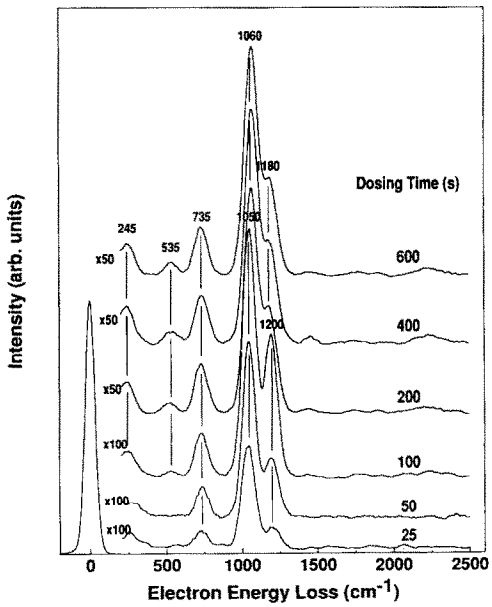

Fig. 9. HREELS spectra as a function of CF_3I exposure on Pt(111) at 103 K (exposures, expressed as dosing times, are indicated on each curve).

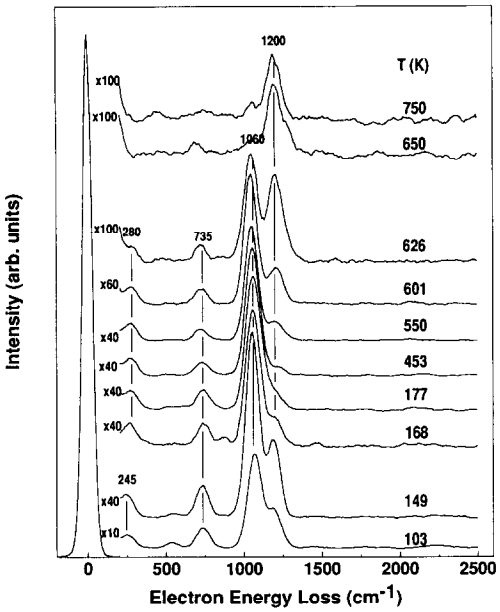

Fig. 10. HREELS spectra for a multilayer CF_3I dosed on Pt(111) at 103 K and then flashed briefly to various temperatures as indicated on each curve. All HREELS spectra were taken after recooling to 103 K.

each curve). Molecular CF_3I features dominate. The observed vibrational modes agree with Raman and infrared spectra of gas-phase CF_3I and with IR data of CF_3I adsorbed on NI(100) [2]. Table 1 lists the possible assignments for the observed bands: 245 for the C–I stretching mode [ν(C–I)], 535 for the asymmetric CF_3 deformation [$\delta_{as}(CF_3)$], 735 for the symmetric CF_3 deformation [$\delta_s(CF_3)$], 1060 and 1180 cm^{-1} for the symmetric and asymmetric C–F stretching modes [ν_s(C–F) and ν_{as}(C–F)], respectively. The C–I stretching mode is about 40 cm^{-1} lower than that in the gas phase, suggesting that the I–P interaction weakens the C–I bond and that CF_3I adsorbs through the I atom. However, as for CH_3I on Pt(111) [13], the Pt–I bonding is too weak to be observed. If the CF_3 group possessed C_{3v} symmetry, the asymmetric modes (e.g. asymmetric deformation and stretching modes at 535 and 1180 cm^{-1}, respectively) would not be seen in dipole scattering. The presence of these models indicates that the C–I axis is tilted with respect to the surface normal.

Fig. 10 shows an annealing set of HREELS spectra for a saturation coverage of CF_3I on Pt(111) (the annealing temperature indicated on each curve). Upon heating, the first significant changes appear at 168 K. The reduced intensities of the asymmetric modes at 535 and 1180 cm^{-1} are consistent with molecular CF_3I desorption and dissociation. A new loss appears at 280 cm^{-1} and exists up to 626 K; the C–I mode disappears. We assign the new mode to rocking [$\rho(CF_3)$] of CF_3 bound to Pt. Since the Pt–Cl stretching mode is at 300 cm^{-1} [14], the Pt–F stretching mode should be slightly higher, but we find no losses in this region. This indicates that atomic F bonded to Pt is not detectable. Between 177 and 453 K, there are no significant changes. That only symmetric modes appear, indicates that the CF_3(a) symmetry must be C_{3v} (D_{3h} can be ruled out because of surface selection rules). At 550 K, a relatively intense loss at 1200 cm^{-1}, assigned to C–F symmetric stretching of CF_2 radicals [15], is

Table 1
Vibrational assignments for CF_3I and CF_3 on Pt(111)

Vibrational mode	CF_3I (Raman) [a] (cm^{-1})	CF_3I (IR) [a] (cm^{-1})	CF_3I/Pt(111) [b] (cm^{-1})	CF_3/Pt(111) [b] (cm^{-1})
$\rho(CF_3)$	265	NR [c]	NR	280
ν(C–I)	284	NR	245	–
$\delta_a(CF_3)$	537	540	535	–
$\delta_s(CF_3)$	741	741	735	735
ν_s(C–F)	1056	1073	1050–1060	1060
ν_a(C–F)	1168	1185	1180–1200	–

[a] Ref. [19].
[b] This work.
[c] NR = not resolved.

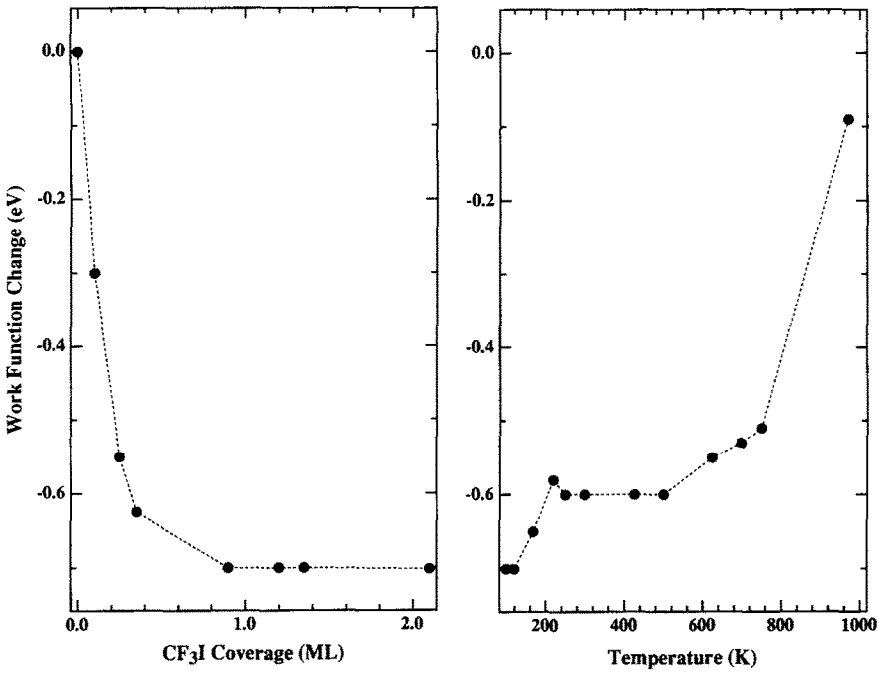

Fig. 11. Work function changes, determined from He(I) UPS secondary electron thresholds, as a function of CF_3I coverage (left panel) and temperature (right panel).

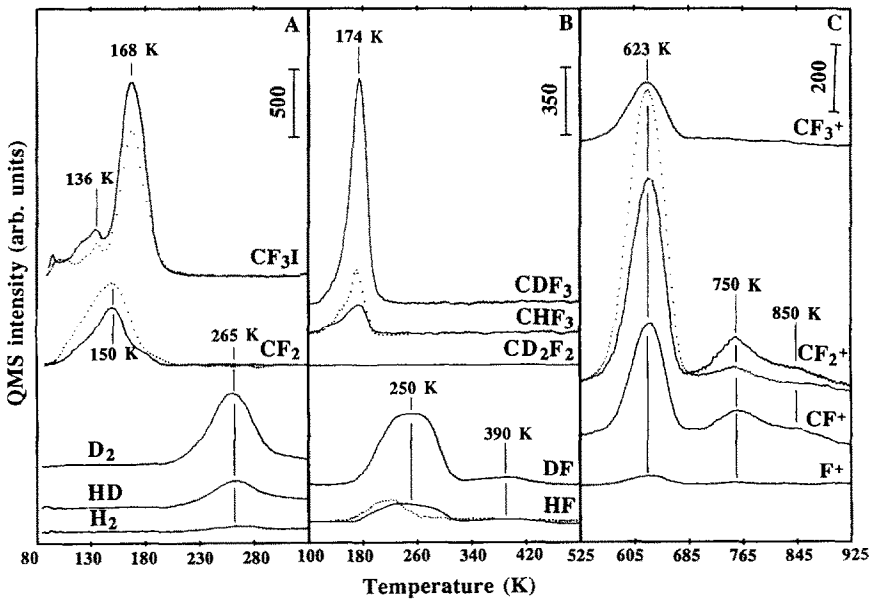

Fig. 12. TPD spectra of different species (indicated on each curve) for 1 ML CF_3I coadsorbed with D(a), 2 L D_2 dose, on Pt(111) at 85 K. The TPD heating rate was 6 K/s. The dashed curves are the corresponding TPD spectra from a D-free surface.

clearly identified. Above 550 K, all the modes (280, 735 and 1060 cm^{-1}) associated with CF_3 lose intensity, while those related to CF_2 intensify. Above 650 K, the loss at 1200 cm^{-1} dominates. Above 800 K, all the losses vanish (not shown). The changes in HREELS above 550 K are consistent with desorption of CF_3 radicals and dissociation of CF_3 to form CF_2. However, we found no evidence for surface atomic F, i.e. no Pt–F stretching mode. This is consistent with XPS results showing that dissociation of CF_3 to form CF_2 is a minor channel for CF_3. As a result, we believe that the amount of F retained is too small to be detected by TPD, XPS or HREELS.

3.1.4. Work function change ($\Delta\phi$)

Fig. 11 shows the work function change ($\Delta\phi$) as a function of CF_3I coverage on Pt(111) (left panel) and, starting with a multilayer coverage, as a function of annealing temperature (right panel). The decrease in ϕ with increasing coverage is ascribed to charge polarization within the oriented CF_3I. Upon heating, the desorption of molecular CF_3I and other species causes a work function increase. Between 240 and 500 K, there is negligible work function change, which is consistent with stable CF_3 dominating the adsorbates. Above 500 K, the desorption and dissociation described above cause an increase in work function. The final rise is due to atomic iodine desorption (due to tiny amounts of I left, the work function of the last point is still slightly lower than that of clean surface).

3.2. CF_3I/D/Pt(111)

Since insight is often gained by isotope labeling, we studied coadsorption of D, prepared by dissociative adsorption of D_2, and CF_3I at 85 K. In TPD, we observed that atomic D activates the C–F bonds in CF_3(a) to form DF around 250 K, resulting in less CF_3 and more CF_2 desorption.

Fig. 12 shows TPD after 1 ML CF_3I was dosed at 85 K on D-covered Pt(111) (2 L D_2). The dotted curves are the corresponding spectra from a D-free surface. Panel A shows desorption of CF_3I, CF_2, and dihydrogen in the temperature region between 80 and 330 K. The interpretation for CF_3I and CF_2 desorption is the same as mentioned above. We attribute the increase in molecular CF_3I desorption to inhibition of CF_3I dissociation by coadsorbed D. Less CF_2 desorption at 150 K supports the interpretation. Surface D and H, the latter mainly from background adsorption, desorb as D_2 and HD at 265 K. Panel B shows TPD spectra of CDF_3, CHF_3, DF and HF. There was no CD_2F_2 desorption. CDF_3 is attributed to hydrogenation of CF_3(a). The absence of CD_2F_2 was expected, since CF_2 desorbs promptly once formed. The DF and HF peaks are unusually broad. We believe that two different F sources contribute to them; the first is dissociation of IF, which we propose is formed in one dissociation channel, and the second is D-induced activation and dissociation of CF_3(a). The latter accounts for the higher temperature portion of DF and HF desorption. The small DF and HF peaks at 390 K are probably due to the decomposition of CDF_x and CHF_x ($x \leq 2$), respectively, because D(a) and H(a) are not available at 390 K. Panel C shows CF_x^+ ($x = 1$–3) and F^+ TPD signals in the temperature region between 525 and 925 K. While CF_3 and I desorption (not shown) intensities decrease, CF_2 radical desorption increases significantly (compare CF_2^+ curves with and without coadsorbed D). These observations suggest that predosed D atoms activate CF_3(a) at about 250 K to produce CF_2 fragments which remain on the surface up to 700 K.

4. Discussion

In this section, we discuss possible reaction mechanisms and surface structures involved in CF_3I on Pt(111). We focus on a multilayer coverage of CF_3I on Pt(111). Scheme 1 outlines the observed results. In scheme 1, the species in ovals are surface bound. Possible reaction channels are shown in scheme 2. In brief, multilayer and a fraction (30%) of monolayer CF_3I desorbs at 100 and 168 K, respectively. Two dissociation channels are proposed for the remaining chemisorbed CF_3I: (i) CF_3(a) and I(a), and (ii) CF_2(g) and IF(a). We suppose that IF(a) is best thought of as a surface complex in which atomic I is strongly

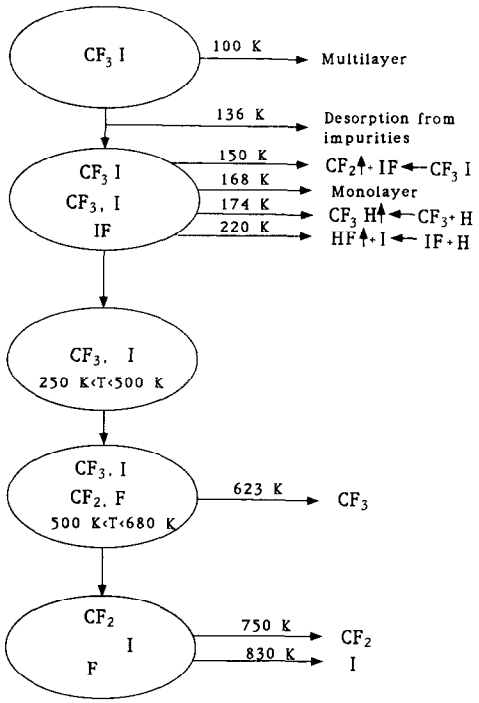

Scheme 1.

perturbed by high electronegative atomic F, and both interact with Pt. Under the influence of the accumulated dissociation products, especially atomic iodine, some CF_3I in the monolayer desorbs at 136 K. For channel (1), a fraction of CF_3(a) reacts with adsorbed background H to form CF_3H, which desorbs at 174 K, while the remaining CF_3(a) changes into a more stable form that is bound very strongly to the substrate and is difficult to hydrogenate, even under high concentration of coadsorbed D. The CF_3(a) desorbs

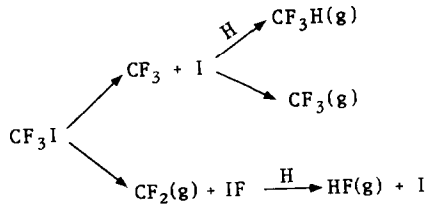

Scheme 2.

(major) and dissociates (minor) into CF_2(a) above 550 K. For channel (2), the CF_2 produced desorbs promptly at the temperature (150 K) where it is formed. IF(a) dissociates and reacts with adsorbed background hydrogen at 220 K to form HF, which desorbs promptly. The atomic iodine desorbs above 800 K.

Evidence that CF_3I adsorbs on Pt(111) through the I atom comes from two sources: (i) the C–I vibrational frequency for adsorbed molecular CF_3I on Pt(111) is lower than for gas-phase CF_3I, and (ii) in passing from submonolayer to multilayer, the F(1s) BE does not change while the I($3d_{5/2}$) does. Since both TPD (inferred from the parent desorption at 136 K) and XPS show evidence of accumulation of atomic I at 135, it is certain that significant C–I cleavage occurs below 135 K. Considering that the onset of CF_2 radical desorption is as low as 100, we suggest that some C–I bond dissociation occurs even at 100 K.

After C–I bond dissociation, two puzzles need to be dealt with. (i) Why do some CF_3(a) species hydrogenate and desorb at 174, while others are not hydrogenated even in the presence of high coverages of D and are stable up to 500 K? (ii) Why do some CF_2 radicals desorb at 150 while others remain to 750 K? We propose two reaction channels as shown in scheme 2. We will discuss them separately.

Hydrogenation of CF_3 to form CHF_3 (or CDF_3) is evident in figs. 4 and 12B. There is only one CHF_3 peak (174 K); the peak temperature does not change with coadsorbed hydrogen coverage (figs. 4 and 12B). Since the CHF_3 signal decays sharply on its high temperature side, we believe that either CF_3(a) or H(a) is completely consumed at about 180 K. Because HF desorption still occurs at 220 and because, when D is coadsorbed, a significant amount of D_2 and HD desorbs at 265 (fig. 12A) and there is still significant CF_3 radical desorption at 623 K (fig. 12C), we conclude that one kind of CF_3(a), rather than H(a), limits the product signal. However, high temperature CF_3 radical desorption indicates that another kind of CF_3(a), more stable and difficult to hydrogenate, exists up to 500 K. Direct evidence is given by HREELS data (fig. 10). Starting at 168 K, a new peak at 280 cm^{-1} appears. Its

presence up to 626 K, along with other characteristic losses, suggests that it belongs to CF_3(a). From 177–453 K, the symmetric stretching and deformation modes of CF_3, as well as the rocking mode, do not change, implying a stable surface structure. The constant work function and F(1s) XPS peak support this notion. Under certain circumstances, e.g. very low coverages or coadsorption with D(a), at least one C–F bond in this stable form of CF_3(a) can be activated as shown in TPD results (fig. 12). The reaction product, HF, desorbs above 250 K, much higher than for CF_3H formation and desorption (174 K). If there were only one kind of CF_3(a), it would be hard to explain why excess surface D cannot hydrogenate all CF_3(a), but can break one C–F bond to produce HF and CF_2. We conclude that there must be a stable form of CF_3(a) existing up to 500 K.

The detailed surface structures of these two kinds of CF_3(a) are not clear. We speculate that, after C–I bond cleavage, most CF_3(a), which can be hydrogenated, occupies either top or bridge sites. During heating, some CF_3(a) moves to hollow sites, causing the surface Pt to move slightly [16] so that the F atom in the CF_3 can interact strongly with Pt. These CF_3(a) fragments are stable and cannot be hydrogenated. The lack of features assignable to CF_2 in both HREELS and XPS rules out the possibility of coexistence of CF_3(a) and CF_2(a) below 500 K. In other words, the CF_2 desorption at high temperatures must be a result of CF_3 dissociation. Stoichiometrically, one F atom is produced for dissociation of every CF_3(a) to form CF_2(a). However, in no case do we find evidence for surface F. As mentioned earlier, this is probably because the amount of F produced is too small to be detected, i.e. dissociation of CF_3(a) is a minor channel, and because atomic F is removed by highly-efficient ESD, as observed for CF_3I on Ru(001) [3].

We now turn to the second question. As discussed above, we propose that high temperature CF_2 radical desorption is the result of CF_3(a) dissociation between 500 and 650, that is, no surface bound CF_2 exists below 500 K (see HREELS results, fig. 10). In the presence of coadsorbed D, some surface bound CF_2 is produced at 250 K via $CF_3(a) + D(a) \rightarrow CF_2(a) + DF(g)$. Clearly, if CF_2 radicals equilibrate with the substrate, they will not desorb thermally below 700 K. Therefore, the CF_2 radical desorption at 150 K comes from some other source. One might argue that the high temperature peaks for CF_2 radicals are due to strongly bound CF_2 and the low temperature peak to weakly bound CF_2. If the latter existed, CF_2H_2 would form and desorb. However, none was found. Because the low temperature CF_2 desorption occurs only at relatively high coverages (> 200 s dose) where molecular CF_3I desorption also takes place, we believe that a crowded surface plays an important role in ejecting CF_2 radicals into vacuum once they are formed. The crowding on the surface prevents this active species from forming a surface bond; it therefore desorbs. However, the CF_2 radical formation and desorption at 150 K must be surface mediated; that is, it does not occur in multilayers. When D is coadsorbed, the Pt is modified or the number of reactive sites are reduced, and less CF_2 desorbs at 150 K (fig. 12b). By way of comparison, low temperature CF_2 radical desorption occurs on Pt(111) and Ni(100) [2], but not on Ag(111) [4] and Ru(001) [3]. No matter how CF_2 forms and desorbs, it must be produced from CF_3I.

On Ni(100) [2], low temperature (~ 220 K) CF_2 radical desorption was attributed to $CF_3(a) \rightarrow CF_2(g) + F(g)$. Here, we propose a different reaction, that is, $CF_3I(a) \rightarrow IF(a) + CF_2(g)$. Based on XPS and HREELS, we ruled out atomic F. Since HF desorption occurs at 130 and the $H(a) + F(a) \rightarrow HF(g)$ reaction occurs at 154 K [5], HF desorption at 220 K is certainly reaction limited, but not by H and F recombination. Rather, we propose that IF forms, accompanying CF_2 radical desorption at 150 K, and dissociates or reacts with H(a) at 220 K to form HF(g) and I(a). Unfortunately, no direct evidence in XPS or HREELS is available to identify IF.

Although both TPD and XPS data indicate that 0.7 ML CF_3I dissociate above 100 K, they do not permit a quantitative discussion of the decomposition yields for different pathways, because some products such as IF and F, though proposed, are not detected. However, we can obtain a lower or upper limit for the dissociation

yields of different pathways. As shown in fig. 6, the low temperature CF_2 radical desorption appears only for doses longer than 200 s. Above 200 s, surface atomic I increases by 0.25, indicating an addition of 0.25 ML CF_3I dissociates. Because, above 200 s, the TPD areas of CF_3 and high temperature CF_2 (750 and 850 K) still increase and CHF_3 desorption appears, it is certain that the yield of low temperature CF_2 radicals (i.e. the $CF_3I \rightarrow CF_2 + IF$ dissociation channel) is not more than 0.25 ML. At saturation, the TPD area of CF_2 desorbed at 750 and 850 K is only 9% of that at 150 K. Therefore, no more than 0.023 ML CF_3 decomposes between 500 and 650 K to form CF_2 and F. The $CF_3I \rightarrow CF_3 + I$ dissociation channel is a major pathway, accounting for at least 0.45 ML CF_3I.

Parenthetically, using schemes 1 and 2, we can reinterpret some data reported previously for CF_3Cl/Pt(111) [5]. Under the influence of 50 eV electrons, CF_3Cl changes the adsorption geometry from bonding through both CL and F to Cl only. Then, thermal activation results in CF_2 radical desorption at 157 K and an HF desorption peak at 270 K, tracking HCl desorption. We believe that FCl forms along with CF_2 desorption and it dissociates and reacts with H(a) to produce HF and HCl (we do not expect HI formation and desorption in the present case).

We now discuss low coverages. Since the coverage onset (200 s dose) for the CF_2 radical, CF_3H and parent CF_3I desorption is the same, we speculate that surface crowding promotes CF_2 and CF_3H formation and desorption. At low coverages, we believe that all the CF_2 and CF_3 remain on the surface and desorb as radicals at high temperatures. Below 50 s dose, adsorbed background hydrogen can activate C–F bonds, resulting in HF formation and desorption, as shown in fig. 4.

It is interesting to compare CF_3 and CH_3 fragments on Pt(111). Both can be hydrogenated by surface H, though at different temperatures, and their thermal stabilities are different: CF_3 is stable up to 500 K while CH_3 dissociates readily below 300 K. This might be traced to the large difference in electronegativity of carbon in the two species leading to a stronger interaction with Pt(111) in the CF_3. Carbon in methyl or other alkyl groups is significantly less electron attracting than hydrogen. Conversely, the CF_3 group is far more electron attracting than hydrogen [17]. Moreover, the C–H bond is weaker than C–F (110 kcal/mol for $H-CH_2$, and 132 kcal/mol for C–F) [18], resulting in easier CH_3 dissociation.

It is still not clear what role atomic I plays. With no I present, CF_3 desorption is more than 100 K lower [5]. On Ru(001), CF_3 and CF_2 [3] desorb before and after atomic I desorption, respectively. On Pt(111), we speculate that atomic I stabilizes surface CF_x. Finally, we point out that CF_3 desorption also is substrate dependent, occurring at 310 on Ag(111) and Ni(100) [2,4], at 623 on Pt(111) and at 705 K on Ru(001) [3].

5. Summary

The work reported here can be summarized as follows:

(i) CF_3I adsorbs molecularly at 85 K with multilayer and monolayer desorption at 100 and 168 K, respectively.

(ii) C–I bond cleavage starts at 100 K and is complete below 220 K.

(iii) There are two competitive reaction channels for CF_3I. One forms $CF_3(a) + I(a)$ and the other forms $CF_2(g) + IF(a)$.

(iv) While part of $CF_3(a)$ can be hydrogenated into CF_3H, which desorbs at 174 K, the remainder transforms into a stable species which is difficult to hydrogenate. Most of the latter desorbs as CF_3 at 623 K, while a small amount dissociates to form CF_2, which desorbs at 750 and 850 K.

(v) While CF_2 desorption, associated with CF_3I dissociation, occurs at 150 K, the IF(a), proposed to be formed concurrently, survives up to 220 K and dissociates into I(a) and F(a), resulting in a reaction limited HF desorption at 220 K.

Acknowledgement

This work was supported in part by the Army Research Office.

References

[1] R.G. Jones and N.K. Singh, Vacuum 38 (1988) 213.
[2] K.B. Myli and V.H. Grassian, Surf. Sci., submitted.
[3] J.S. Dyer, P.A. Thiel, Surf. Sci. 238 (1990) 169.
[4] M.E. Castro, L.A. Pressley, J. Kiss, S.K. Jo, X.-L. Zhou and J.M. White, J. Phys. Chem., submitted.
[5] J. Kiss, D.J. Alberas and J.M. White, Surf. Sci. 275 (1992) 82.
[6] G.E. Mitchell, P.L. Radloff, C.M. Greenlief, M.A. Henderson and J.M. White, Surf. Sci. 183 (1987) 403.
[7] S.K. Jo, X.Y. Zhu, D. Lennon and J.M. White, Surf. Sci. 241 (1991) 231.
[8] EPA/NIH Mass Spectral Data Base, Eds. S.R. Heller and G.W.A. Milne (US Government Printing Office, Washington, 1978).
[9] E. Bechtold, Appl. Surf. Sci. 7 (1981) 231.
[10] F.T. Wagner and T.E. Moylan, Surf. Sci. 182 (1987) 125.
[11] B. Roop, S. Joyce, J.C. Schultz and J.I. Steinfeld, J. Chem. Phys. 83 (1985) 6012.
[12] A. Bensaoula, E. Grossman and A. Ignatiev, J. Appl. Phys. 62 (1987) 4587.
[13] M.A. Henderson, G.E. Mitchell and J.M. White, Surf. Sci. 184 (1987) L325.
[14] V.H. Grassian and G.C. Pimentel, J. Chem. Phys. 88 (1988) 4484.
[15] M.E. Jacos, J. Phys. Chem. Ref. Data 13 (1984) 945.
[16] J.T. Yates, Jr., Chem. Eng. News (1992) 22.
[17] J.D. Roberts and M.C. Caserio, Basic Principle of Organic Chemistry, 2nd ed. (Benjamin, New York).
[18] R.C. Weast, M.J. Astle and W.H. Beyer, CRC Handbook of Chemistry and Physics (CRC Press, Boca Raton, 1986).
[19] W.F. Edgell, C.E. May, J. Chem. Phys. 22 (1953) 1808.